Middle-East Journal of Scientific Research 17 (5): 600-606, 2013
ISSN 1990-9233

DOI: 10.5829/idosi.mejsr.2013.17.05.12210

Flue Gas Desulfurization Utilizing Limestone Particles: A CFD Modeling

Leila Vafajoo, SoroushSabbaghian and Behrooz Beigy

Chemical and Environmental Engineering Group,
Islamic Azad University, Tehran South Branch, Ahang Blvd., Tehran, Iran

Abstract: SO_2 emissions from different industrial activities including production of electricity from power plants as well as, metallurgical and cement factories, to name a few, are undesired due to this chemical's harmful effects. Many processes to reduce sulfur dioxide emissions have been developed. Amongst these processes, direct dry sorbent injection is a relatively simple and low-cost process. In the current study, a two dimensional CFD investigation of the direct sulfatesorption from a flue gas utilizing limestone was presented. This model accounted for the process taking place in a fixed bed reactor. Effects of important operating parameters including; the temperature, SO_2concentration and gas velocity were studied in this work. Direct sulfation was revealed to be controlled by both the chemical reaction as well as, diffusion phenomena. Consequently, thetemperature overwhelmingly affected this process.Moreover, the maximum conversion of $CaCO_3$accured

Key words: Flue gas · Direct Sulfation · Computational Fluid Dynamics · Fixed-bed

INTRODUCTION

Nowadays, it is well known that SO_2 is one of important greenhouse gases. SO_2 is emitted from different industrial activities and causes adverse and harmful environmental effects. Industries emitting SO_2 include power production, the metallurgical industries as well as, cement producing factories. During the past decades, extensive works have been performed to prevent SO_2 emissions. Various processes have been developed for cleaning of the flue gases from the sulfur, including wet scrubbing, dry scrubbing, direct dry sorbent injection and regeneration processes [1]. Amongst all these processes, direct dry sorbent injection is a relatively simple and low-cost process. In this process, the sorbent, often limestone, is injected directly into the process at a place where the absorption of SO_2 on the sorbent may readily occur, for example, the combustion chamber in power plants. With limestone as the sorbent, the sulfation reaction may proceed via two different routes depending on whether calcination of the limestone took place under specific reaction conditions or not. The dissociation of limestone is normally determined by the CO_2 partial pressure in the system. Limestone decomposes to form CaO and CO_2 when the partial pressure of CO_2 in the system is lower than its equilibrium value over the limestone at the same temperature.

If calcination of the limestone took place under such conditions that the CO_2 partial pressure in the system was lower than its equilibrium value over the limestone, the limestone would first decompose into the CaO form. The CaO then reacted with SO_2. This process is referred to as the indirect sulfation reaction and is expressed by the following overall reactions [1, 2]:

$$CaCO_3(s) \rightarrow CaO(s) + CO_2(g) \quad (1)$$

$$CaO(s) + SO_2(g) + 0.5O_2(g) \rightarrow CaSO_4(s) \quad (2)$$

If calcination of the limestone does not take place, in other words, the CO_2 partial pressure in the system is higher than its equilibrium value over the limestone then this species may react directly with SO_2. This process is often called the direct sulfation reaction and is expressed by the following overall reaction:

$$CaCO_3(s) + SO_2(g) + 0.5O_2(g) \rightarrow CaSO_4(s) + CO_2(g) \quad (3)$$

Corresponding Author: Leila Vafajoo, Chemical and Environmental Engineering Group,
Islamic Azad University, Tehran South Branch, Ahang Blvd. Tehran, Iran.

The direct sulfation reaction might be significantly influenced by various parameters, such as temperature, system pressure and gas concentrations. The degree of influence of each of these parameters on the direct sulfation reaction varies with the reaction conditions.

Lisa *et al*. [3] suggested that the low reaction order of SO_2 that they observed at high conversions was related to solid-state diffusion control. Spartinos *et al*. [4] believed that the high reaction order they observed was due to a possible increase of the micro-porosity of the product layer with the increase of the SO_2 concentration caused by the faster evolution of the CO_2 gas at higher SO_2 concentrations.

Qiu *et al*. [5] investigated the effect of the system's pressure in a PTGA by maintaining constant partial pressures of SO_2 and CO_2. The oxygen content in the gas was 5%. It was observed that the rate of the sulfation reaction at 1123 K was significantly lowered at higher pressures despite the increase of oxygen concentrations. The effective diffusive in the product layer was also evaluated to be lower at higher system pressures. These authors suggested that the effect of the higher system pressures was caused by possible structure variation of the product layer or increased resistance of the outward diffusion of the formed CO_2. Bulewicz *et al*. [6] investigated the effect of the system pressure at constant gas composition in terms of volume percentage. In this case, the gas concentrations were increased with the increase of the system pressure.

The experimental observations of Illerup *et al*. [7], Hanson *et al*. [8] and Zevenhoven *et al*. [9] clearly demonstrated that the sintering of limestone at high temperatures and its consequence for the sulfation reaction. Hanson *et al*. [8] studied the sintering of calcium carbonate in a tube furnace in 100% CO_2 gas at atmospheric pressure. It was observed through the SEM that sintering of the particles of $CaCO_3$ started at about 973 K. The negative influence of the sintering of limestone particles on the sulfation reaction is well demonstrated by the observations of Illerup *et al*. [7] as well as Zevenhoven *et al*. [9]. Illerup *et al*. [7] studied the direct sulfation reaction in a pressurized fixed-bed reactor at 1023 K with Stevns Chalk, a porous limestone. The particle size was 0.85–1 mm. It was observed that the limestone particles lost partly their reactivity after a heat treatment at 1123 K.

It is seen that there is a definite need for a mass transfer model which might be capable of providing a general methodology for simulation of the direct sulfation of SO_2 in a fixed bed reactor. The main purpose of the current study is to develop a mass transfer model for calculation of SO_2 concentration in fixed bed reactor. The mass transfer model developed here is 2 dimensional taking into account axial and radial diffusion mass transfer in the reactor. The model also considers momentum transfer in the reactor. The model predictions are validated utilizing experimental values reported in literature [10-12].

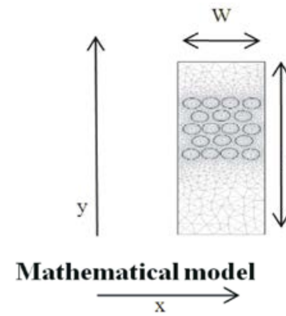

Fig. 1: Model domain and Meshes utilized in the present simulations

Mathematical Modeling: The sulfation of limestone is a very complicated process. Some parameters such as effective diffusivity are very difficult to obtain directly. Mathematical modeling is indeed necessary to investigate this process. Simplifying assumptions for this purpose are as follows:

- The system is isothermal;
- The reaction is irreversible, single and first order (with respect to SO_2 concentration at the surface of the un-reacted core) with an Arrhenius-type dependence on temperature;
- The diffusivity inside the product layer is uniform;
- The particle is spherical;
- The overall particle size does not change during reaction;
- There is no reaction inside the un-reacted core and
- The O_2 molecule has no effect on sulfation when its concentration is above 5%.

Fig. 1 shows the model domain and meshes for the mass and momentum transfer equations.

Gas Phase Equations: The unsteady mass conservation equation in the product layer is given as follow:

$$\partial C_i / \partial t + \nabla.\left(-D_i \nabla C_i + C_i U\right) = R_i \tag{4}$$

With respective boundary conditions provided by:

At y = L $\quad C = C_0$

At y = 0 $\quad n.(-D_i \nabla C_i) = 0$

At x = 0 $\quad \frac{\partial C_i}{\partial x} = 0$

At x = w $\quad \frac{\partial C_i}{\partial x} = 0$

Here, the C_i is the SO_2 molar concentration (mol/m^3); C_0 is the SO_2 molar concentration in the bulk of the gas (mol/m^3); D_i is the effective diffusivity of SO_2 in the product layer (m^2/s) and k_s is the reaction rate constant on area basis (m/s).

By solving this equation, the distribution of gas concentrations (SO_2) released during the reactor is determined. To solve the continuity equation, momentum equation required to determine the velocity distribution. The Nervier-Stokes equation determined the velocity distribution in the gas phase, in other words;

$$\frac{\rho \partial U}{\partial t} - \nabla.\left[-pl + \eta\left(\nabla U + (\nabla U)^T\right) + \rho(U.\nabla)U + \nabla P = F\right. \tag{5}$$

$$\nabla.U = 0 \tag{6}$$

Here, P is the system's pressure (Pa), U is the gas velocity, t is the time, η is the dynamic viscosity and F is the volume force.

Boundary conditions of the Navier-Stokes equation considered as follow:

At y = L $\quad U = U_0$

At y = 0 $\quad P = P_{atm}$

At x = 0 $\quad U = 0$

At x = w $\quad U = 0$

By solving equations of continuity and Navier-Stokes simultaneously, the concentration distribution in the gas phase was determined.

Flow Equations Inside the Porous Spherical Particles of Lime: Continuity equation within the spherical particles is defined as follow:

$$\partial C_i / \partial t + \nabla.\left(-D_j \nabla C_j + C_j U\right) = R_i \tag{7}$$

Respective boundary condition for the Continuity equation is as follow:

At $r = r_0$ $C = C_{bulk}$

Table 1: Constants used in the present simulations [2]

Parameter	value	Unit
K_0	19	m/s
E	90000	J/mol
R	8.314	J/mol.K
T	1123	K

Table 2: Constants used in the present simulations [2]

Parameter	Value	Unit
SO_2 Density	0.66	Kg/m^3
SO_2 Viscosity	2.6*10-5	Pa.s
Effective diffusivity of SO_2 in particles	6.71*10-6exp(-10000/T)	m^2/s
Diffusivity of SO_2 in gas film	2.49*10-8	m^2/s
O_2 concentration in gas feed	0.2	m^3
Total gas flow rate	1*10-4	m^3/s
Total pressure	1.013*105	Pa
Sample weight	0.2	gr
Temperature	1123	K

Table 3: Fixed bed parameters used in the present simulations [2]

Parameter	Value	Unit
Particle size	54	mµ
Reactor inner diameter	0.02	M
Reactor length	0.65	M
Porosity of part-filled of the bed	0.41	-

Chemical reaction occurred inside the spherical particles between sulfur dioxide and spherical particles of $CaCO_3$. The observed reaction which reduced the sulfur dioxide gas stream at the output was of apparent first order in SO_2. Thus, the kinetics of the reaction was as follows:

$$-r_a = k * C_{so2} \tag{8}$$

By using Arrhenius equation, reaction rate constant was determined:

$$k = k_o \exp\left(-\frac{E}{RT}\right)$$

Kinetic parameters are presented in Table 1.

Tables 2 and 3 show the parameters utilized in the present simulations.

Numerical Solution of Governing Equations: The model equations related to gas and particles phases with the appropriate boundary conditions were solved using by finite element method (FEM) for numerical solutions of the governing model equations. The finite element analysis was combined with adaptive meshing and error control.

RESULTS AND DISCUSSIONS

Velocity Distribution of Gas Inside the Bed: Fig. 2 shows gas velocity distribution in the bulk. Fluid velocity distribution obtained from Navier-Stocks equations. As may be seen from this figure, the velocity changed in the free flow was not sensible however; it changed significantly near the solid walls of porous spherical particles. This is due to the viscous forces exerted by the solid wall which led to creation of severe velocity gradient around the dead spots and some porous spherical particles.

Concentration Distribution of Gas Flow Inside the Bed: Fig. 3 shows concentration distribution of sulfur dioxide in the bed including gas stream and porous spherical particles. The gas mixture containing SO_2/O_2 flew from the side of the bed (y = L) where the concentration of SO_2 was the highest. As the SO_2 flew through the bed, it was transferred toward the particles due to the concentration difference (*i.e.*; driving force). Mechanisms of the mass transfer in the bulk were convection and diffusion. In the y-direction the predominant mass transfer mechanism was the convection since the fluid flew in this direction, while in the x-direction, diffusion occurred due to large concentration differences. The SO_2 gas is transferred through the particle only by diffusion mechanism and then reacts with the particles.

However, concentration gradient created in the bed was due to the chemical reaction and reduced concentration of the SO_2. Furthermore, this figure showed that the chemical reaction on the spherical particles was relatively fast such that the concentration of sulfur dioxide on the center of the spheres almost reached zero.

SO_2 Concentration Distribution Inside the Porous Spherical Particles: Fig. 4 shows concentration distribution of the SO_2 inside the spherical particles. Samples of particles were chosen at the top, middle and bottom of the reactor respectively and time scale was set between 0-5000 seconds. This figure showed reduction of sulfur dioxide concentrations at different times and locations through the porous spherical particles. The governing equation in the particles was the Fick's law of diffusion. This figure also revealed that the reaction between the SO_2 and particle's surface was so fast such that the gas might have not reached the core of the particles.

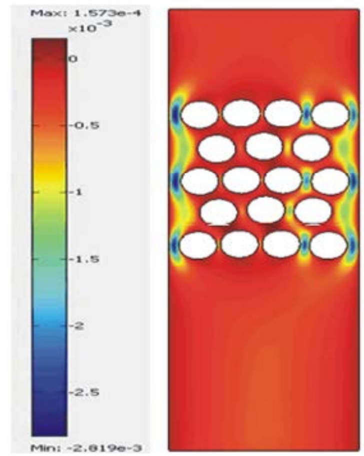

Fig. 2: Velocity distribution of gas inside the bed for the present study

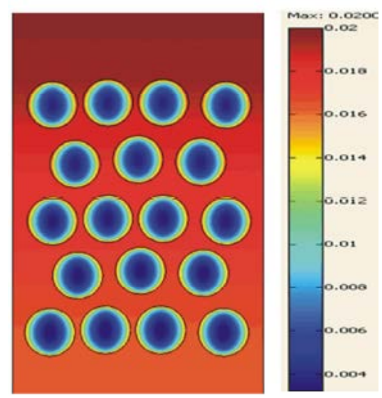

Fig. 3: Concentration distribution of the SO2 gas in the fixed bed investigated in

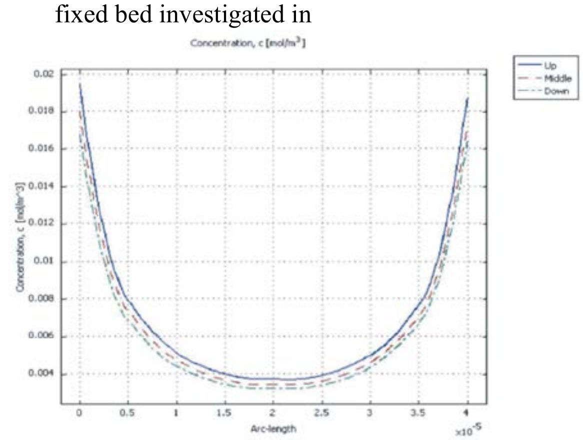

Fig. 4: Concentration distribution of the SO2 gas inside the spherical particles

Investigation on Concentration Changes along the Reactor: Concentration changes for the SO_2 species along the reactor are illustrated in Fig. 5. This shows the

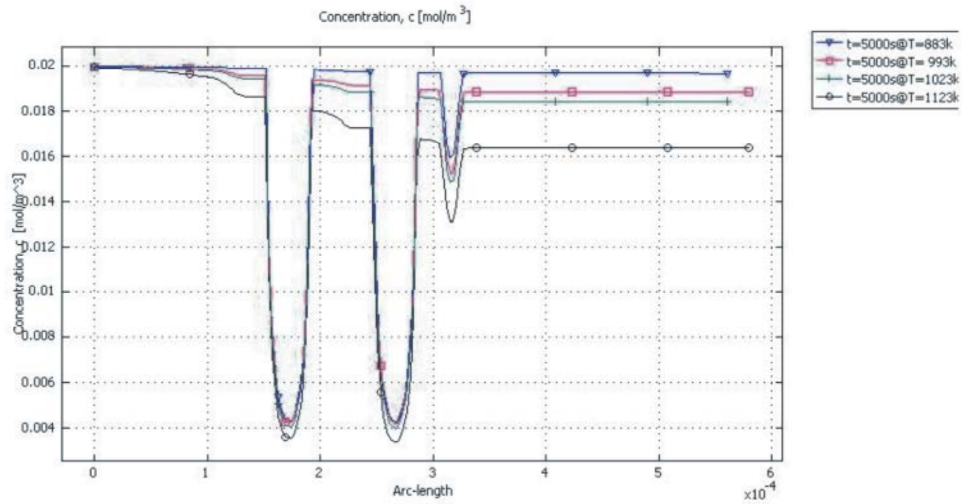

Fig. 5: Concentration changes along the reactor in steady state condition (t = 5000 s)

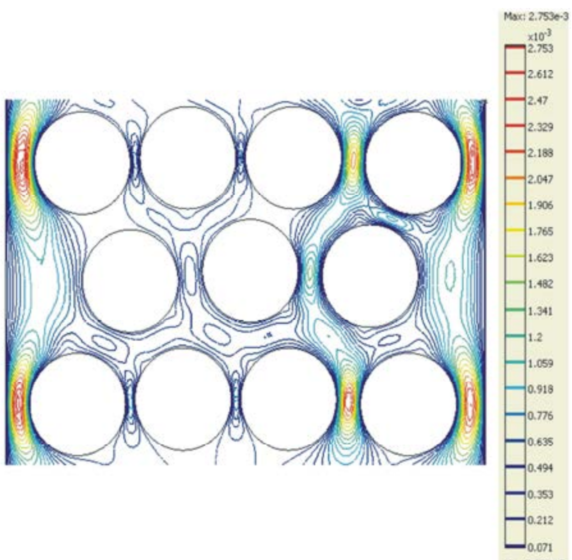

Fig. 6: Velocity contours along the reactor and around the solid particle

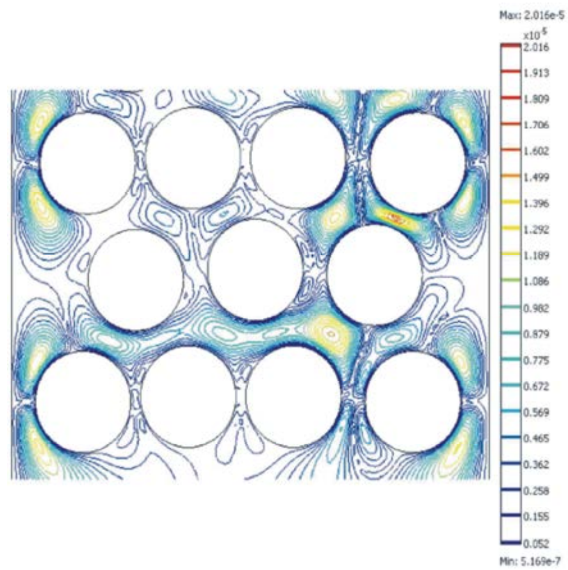

Fig. 7: Concentration contours along the reactor and around the solid particle

concentration variations for different temperature after the system becomes stable (*i.e.*; after 5000 seconds). This figure clearly indicated that there were some minimums in the resulting curve due to porous particles in the bed. Also it was revealed that with increasing temperature, the concentration loss was enhanced in the bed and might have given rise to an increase in the conversion. This was attributed to the fact that with increased temperature, the reaction rate between particles and SO_2 as well as, the SO_2 diffusivity in the gas phase rose which in turn resulted in reduction of the SO_2 concentration in the bed (Figure 6). Data presented in this figure showed that the simulation findings were in good agreement with the experimental data.

Investigation of Velocity and Concentration Contour along the Reactor: Figs. 6&7 show velocity and concentration contours along the reactor. Velocity contours along the reactor and around the solid particles (limestone) are illustrated in Fig. 6. As it can be seen, minimum velocity occurs near the wall and also between

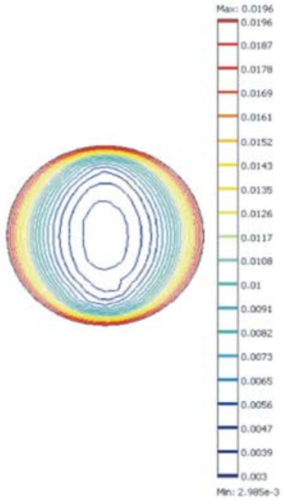

Fig. 8: Concentration contours inside the solid particle

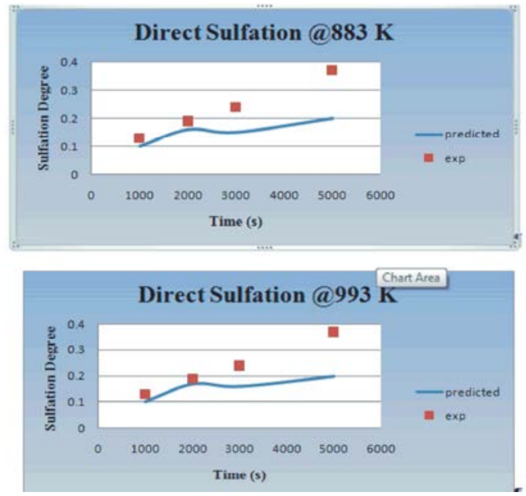

Fig. 9: Comparison between experimental and simulation results

the particles that their distance is too low. Also from Fig. 6 it is deduced that flow tends to deviate towards wall of the reactor and can be observed restricted flow and dead spots in some regions in the reactor.

Fig. 7 shows concentration contours along the reactor. The same trend can be observed for concentration contours. Fig. 7 also represents that the concentration distribution of SO_2 along the reactor is not uniform. This could be attributed to random packing of solid spheres in the reactor.

Investigation of Concentration Contour for a Particle: Fig. 8 indicates the concentration contours in a solid particle. Significant point in this figure is that, whatever flows into the solid particle along processing time, concentration gradient decreases and at the center of the particle concentration gradient approximately can be considered zero. Also it can be observed that concentration gradient at different areas of particle is not uniform. It is observed that at the surface of particle, concentration gradient is significant because of high reaction rate. Furthermore, it implies that the chemical reaction is not instantaneous and the assumption of first order reaction is valid here and can be observed from figure.

Model Validation: To ensure the accuracy of the developed model, the simulation results were compared with experimental data reported in the literature [6]. Fig. 9 indicates comparisons between these data for the case of different temperature. Four temperatures were considered in the simulations. Through this figure, the sulfation degree was compared. Sulfation degree is calculated from the reaction time as follows [2]:

$$X = \varepsilon 0 - \frac{\varepsilon}{(z-1)(1-\varepsilon 0)} \tag{10}$$

where, X is the sulfation degree, ε is the porosity, ε_0 is the initial porosity and z is the ratio of molar volume of solid phase after reaction to that before sulfation reaction.

Fig. 9 confirms that the simulation results are in good agreement with the experimental data. It also reveals that for higher temperature, the model predicts the reactor performance much better. Therefore, the optimum temperature can be chosen 1123 K which is in accordance with the literature and experimental works [2].

CONCLUSION

A two dimensional comprehensive mass transfer model was developed to study the direct sulfation of the SO_2 in a fixed bed reactor. This model was based upon simultaneously solving the conservation equations including mass and momentum transfer for the SO_2 species in the bulk and through porous particles. The model equations were solved numerically using the CFD technique based upon finite element method (FEM). It was found that during the direct sulfation both the chemical reaction and diffusion were presented and limiting. The diffusivity in the product layer demonstrated high temperature dependence while hardly depended upon the sulfation degree. It was shown that the direct sulfation reaction may be significantly affected by all of the gaseous reactants and products. The degree of influence of each gas varied with reaction conditions. Higher CO_2 concentrations significantly hindered the direct sulfation reaction. On the other hand, it was shown that higher temperatures adversely affected this reaction. Furthermore, the theoretical findings were compared with experimental data reported in the literature and determined to be in good agreement with one another. Results obtained from this research revealed that the developed model was appropriate and reasonably accurate for prediction of direct sulfation of the SO_2 in a fixed bed reactor. Ultimately, this research provided a complementary theoretical method to an existing experimental technique the former of which might be utilized for further process optimizations.

Nomenclature:

- C = SO_2 molar concentration (mol/m^3)
- C_0 = SO_2 molar concentration in bulk gas (mol/m^3)
- D = Diffusivity of SO_2 in gas film (m^2/S)
- D_e = Effective of diffusivity of SO_2 in product layer (m^2/s)
- D_{e0} = Initial effective diffusivity of SO_2 in product layer during CaO-SO_2sulfation (m^2/s)
- k = Reaction rate constant on apparent area basis (m/s)
- k_0 = Initial rate constant
- r = Particle radius (m)
- r_0 = Initial particle radius (m)
- R = Universal gas constant (J/mol K)
- t = Reaction time (s)
- T = Temperature (k)
- X = Sulfation degree (molar fractional conversion of CaO from $CaCO_4$)
- F = Volume force (kg/m^2 s^2)
- E = Activation energy (J/mol)
- P = System pressure (Pa)
- z = Ratio of molar volume of solid phase after reaction to that before reaction
- ε = Porosity
- ε_0 = Initial porosity
- ρ = Particle density (mol/m^3)
- η = Dynamic Viscosity (Pa.s)

REFERENCES

1. Hu, G., K. Dam-Johansen, S. Wedel and J. Peter Hansen, 2006. Review of the direct sulfation reaction of limestone. Progress in Energy and Combustion Science, 32(4): 386-407.
2. Liu, H., S. Katagiri, U. Kaneko and K. Okazaki, 2000. Sulfation behavior of limestone under high CO_2 concentration in O_2/CO_2 coal combustion. Fuel, 79(8): 945-953.
3. Iisa, K., M. Hupa and P. Yrjas, 1992. Product layer diffusion in the sulphation of calcium carbonate. Symposium (International) on Combustion, 24(1): 1349-1356.
4. Spartinos, D.N. and C.G. Vayenas, 1991. Kinetics of sulphation of limestone and precalcined limestone. Chemical Engineering and Processing: Process Intensification, 30(2): 97-106.
5. Qiu, K. and O. Lindqvist, 2000. Direct sulfation of limestone at elevated pressures. Chemical Engineering Science, 55(16): 3091-3100.
6. Bulewicz, E.M., S. Kandefer and C. Jurys,1986. Desulphurization during the fluidized combustion of coal using calcium-based sorbents at pressures up to 600 kpa. Journal of the Institute of Energy, 59(441): 188-195.
7. Illerup, J.B., K. Dam-Johansen and K. Lundén, 1993. High-temperature reaction between sulfur dioxide and limestone—VI. The influence of high pressure. Chemical Engineering Science, 48(11): 2151-2157.
8. Hanson, C. and C. Tullin, 1996. Sintering of calcium carbonate and lime mud in a carbon dioxide atmosphere. Journal of Pulp and Paper Science, 22(9): J327-J331.
9. Zevenhoven, R., P. Yrjas and M. Hupa, 1998. Sulfur dioxide capture under PFBC conditions: the influence of sorbent particle structure. Fuel, 77(4): 285-292.
10. Sokeng, S.D., D. Lontsi, P.F. Moundipa, H.B. Jatsa, P. Watcho and P. Kamtchouing, 2007. Hypoglycemic Effect of Anacardium occidentale L. Methanol Extract and Fractions on Streptozotocin-induced Diabetic Rats, Global Journal of Pharmacology, 1(1): 01-05.
11. Prajapati Hetal Ritesh, Brahmkshatriya Pathik Subhashchandra, Vaidya Hitesh Bharatbhai and V. Thakkar Dinesh, 2008. Avian Influenza (Bird Flu) in Humans: Recent Scenario, Global Journal of Pharmacology, 2(1): 01-05.
12. Okafor, P.N., K. Anoruo, A.O. Bonire and E.N. Maduagwu, 2008. The Role of Low-Protein and Cassava-Cyanide Intake in the Aetiology of Tropical Pancreatitis, Global Journal of Pharmacology, 2(1): 06-10.